European Journal of Neuroscience, Vol. 23, pp. 1142–1150, 2006 doi:10.1111/j.1460-9568.2006.04660.x

Transient expression of A-type K^+ channel α subunits Kv4.2 and Kv4.3 in rat spinal neurons during development

Hsin-Yi Huang, Chien-Wei Liao, Pei-Hsuan Chen and Meei-Ling Tsaur
Institute of Neuroscience, National Yang-Ming University, Taipei, Taiwan 112, Republic of China

Keywords: development, intermediate gray interneurons, rat, somatic motoneurons, visceral motoneurons

Abstract

A-type K^+ currents (I_As) have been detected from the ventral horn neurons in rat spinal cord during embryonic day (E) 14 to postnatal day (P) 8 but not in adulthood. It is not known which types of neurons and which A-type K^+ channel α subunits express the I_As and what the possible function might be. Here, we examined the expression of two A-type K^+ channel α subunits, Kv4.2 and Kv4.3, in rat spinal cord at various developmental stages by immunohistochemistry. We found a transient expression of Kv4.2 in somatic motoneurons during E13.5–P8 with a peak around E17.5, which coincides temporally with the natural selection of motoneurons. Transient expression of Kv4.2 and Kv4.3 was also observed in the intermediate gray (IG) interneurons. During E19.5–P14, some IG interneurons express Kv4.2, some express Kv4.3 and a subset co-express Kv4.2 and Kv4.3. Peak expression of Kv4.2 and Kv4.3 in the IG interneurons was detected around P1, which coincides temporally with the developmental selection of IG interneurons. In contrast to the I_A-expressing subunits Kv4.2 and Kv4.3, a delayed-rectifier K^+ channel α subunit Kv1.6 is persistently expressed in somatic motoneurons and IG interneurons. Together, these data support the hypothesis that expression of I_As may protect I_A-expressing somatic motoneurons, and possibly also IG interneurons, from naturally occurring cell death during developmental selection.

Introduction

A-type K^+ currents (I_As), which provide fast repolarization to prevent the firing of action potentials, are crucial in the control of neuronal excitability (Hille, 2001; reviewed in Toledo-Rodriguez *et al.*, 2005). The physiological roles of I_As in mature neurons have been extensively studied (reviewed in Pongs, 1999), whereas their roles in immature neurons remain unclear. In rat spinal cord, I_As have been detected in the somatodendritic domain of ventral horn neurons from embryonic day (E) 14 to postnatal day (P) 8 but not in adulthood (reviewed in Perrier & Hounsgaard, 2000). Cell bodies of somatic motoneurons and the majority of intermediate gray (IG) interneurons are located in the ventral horn. It is not known which types of neurons and which A-type K^+ channel α subunits express the I_As and what the possible function might be.

So far there are five I_A-expressing subunits in mammals: Kv1.4, Kv3.4, Kv4.1, Kv4.2 and Kv4.3 (reviewed in Coetzee *et al.*, 1999). In neuronal cultures derived from E14 rat ventral horn, Kv4.2 and Kv4.3 mRNAs are most abundant, Kv1.4 and Kv4.1 mRNAs are at low levels, whereas Kv3.4 mRNA is barely detectable (Alessandri-Haber *et al.*, 2002). Kv4.2 and Kv4.3 are the major contributors of I_As recorded from the somatodendritic domain of all central nervous system neurons examined. In contrast, Kv1.4 and Kv3.4 appear more frequently in the axons and nerve terminals (Veh *et al.*, 1995; Birnbaum *et al.*, 2004; Rhodes *et al.*, 2004; Huang *et al.*, 2005). The subcellular localization of Kv4.1 in central nervous system neurons remains unknown. Thus, it is likely that Kv4.2 and/or Kv4.3 contribute to the I_As detected from the somatodendritic domain of ventral horn neurons during E14–P8. In addition to Kv4.2 and Kv4.3 mRNAs, abundant Kv1.6 mRNA has been detected from the E14 rat ventral horn neuronal cultures (Alessandri-Haber *et al.*, 2002). In contrast to Kv4.2 and Kv4.3, Kv1.6 evokes delayed rectifier K^+ currents in heterologous expression systems (Coetzee *et al.*, 1999).

In this report, to investigate whether the I_A-expressing subunits Kv4.2 and Kv4.3 contribute to the I_As detected from rat ventral horn neurons during E14–P8, we examined their cellular and subcellular localization in rat spinal cord at various developmental stages. The expression of delayed rectifier K^+ current-expressing subunit Kv1.6 was also examined for comparison.

Materials and methods

Animals

Sprague-Dawley rats [P1, P8, P14 and adulthood (8–10 weeks)] and embryos in pregnant females (E12.5, E13.5, E15.5, E17.5 and E19.5) were provided by the Animal Center, National Yang-Ming University. National guidelines on animal care were followed and all the experiments were approved by the local ethics committee of the National Yang-Ming University. The day of birth was defined as P1. Timed pregnancies were established by checking for vaginal smears on the morning following mating. We designated noon on the day sperm were detected as E0.5.

Perfusion

Postnatal rats were injected intraperitoneally with 4000 units of heparin/kg body weight to prevent blood clotting. After 5 min,

Correspondence: Dr Meei-Ling Tsaur, as above.
E-mail: mltsaur@ym.edu.tw

Received 31 August 2005, revised 8 December 2005, accepted 30 December 2005

animals were anesthetized by injection of sodium pentobarbital (120 mg/kg) and perfused transcardially with normal saline followed by 4% paraformaldehyde in phosphate-buffered saline (PBS) and 2% paraformaldehyde for Kv4.2 staining. Cervical and thoracic segments of the spinal cord were removed and postfixed with 4% paraformaldehyde in PBS at room temperature (25 °C) for 30 min in P8–P14 rats or 1 h in adult rats. Embryos were removed from dams, perfused with 4% paraformaldehyde in PBS and immersed in the same fixative at 4 °C for 30 min. All specimens were cryo-protected in 30% (w/v) sucrose in 0.1 M phosphate buffer (pH 7.4) with two changes.

Single antigen immunohistochemistry

Kv4.2 and Kv4.3 polyclonal antibodies purified from rabbit sera were purchased from Alomone Laboratories (Jerusalem, Israel) and the specificity has been confirmed previously (Hsu *et al.*, 2003; Huang *et al.*, 2005). Spinal cords were cut with a cryostat into 20–35-μm sections in transverse orientation. Sections from embryos were mounted directly onto gelatin-coated slides, whereas sections from postnatal rats were processed in a floating manner. After washing in PBS, followed by washing in PBS containing 0.3% Triton X-100 (PBST) twice for 10 min, sections were treated with 0.3% hydrogen peroxide in PBST for at least 15 min to exhaust the endogenous hydrogen peroxidase. Non-specific binding was blocked by 3% normal goat serum plus 2% bovine serum albumin in PBST for 1 h for floating sections or 2 h for sections on slides. Sections were incubated at room temperature overnight with primary antibody in PBST plus 3% normal goat serum. The primary rabbit polyclonal antibodies and their dilution factors applied to floating sections were anti-Kv4.2 (1 : 300), anti-Kv4.3 (1 : 200) and anti-Kv1.6 (1 : 100; Alomone Laboratories), respectively. Concentrations of primary antibodies were doubled for sections on slides. Sections were washed three times for 5 min each with PBST and incubated with goat anti-rabbit biotinylated secondary antibody (1 : 1000; Pierce, Rockford, IL, USA) for 1.5 h at room temperature. After washing three times with PBST, avidin-biotin-horseradish peroxidase complex (Pierce) in PBS was applied in a 1 : 150 dilution to floating sections for 1 h or in a 1 : 80 dilution to sections on slides for 1.5 h. Antigens were visualized by combining equal volumes of an ammonium nickel sulfate solution (30 mg/mL in 0.1 M sodium acetate, pH 6.0) and a diaminobenzidine solution (4 mg/mL in PBS) in the presence of 0.01% hydrogen peroxide. Floating sections were spread flat on slides, air-dried, rinsed with distilled water for 1 min and dehydrated through an ethanol gradient (70% once, 95% twice and 100% twice) for 1.5 min each and then twice in xylene for 3 min. Sections were coverslipped with the mounting medium Permount (Merck, Darmstadt, Germany). Images were acquired with a DMX1200 digital camera connected to an Eclipse E800 light microscope (Nikon, Melville, NY, USA) and processed with PHOTOSHOP 8.0 software (Adobe, Mountain View, CA, USA).

Double antigen immunofluorescent staining

The following procedure was used for double staining with two antibodies derived from different species. Sections were processed similarly to the description in 'Single antigen immunohistochemistry', except that treatment with hydrogen peroxide was omitted. Sections were incubated simultaneously with anti-Kv1.6 (1 : 50), anti-Kv4.2 (1 : 150) or anti-Kv4.3 (1 : 100) antibody with one of the following primary antibodies. Mouse monoclonal antibodies included anti-calretinin (1 : 100; Chemicon, Temecula, CA, USA), anti-Islet1/2 (1 : 200) (Developmental Studies Hybridoma Bank, University of Iowa, Iowa City, IA, USA) and anti-microtubule-associated protein-2 (MAP2) (1 : 100; Sigma, St Louis, MO, USA). Goat antibodies anti-calbindin (1 : 50; Santa Cruz Biotechnology, Santa Cruz, CA, USA) and anti-choline acetyltransferase (ChAT) (1 : 100; Chemicon) were also used. Secondary antibodies included Alexa Fluor 488-conjugated donkey anti-rabbit IgG (1 : 500; Molecular Probes, Eugene, OR, USA), Alexa Fluor 594-conjugated donkey anti-mouse IgG (1 : 500; Molecular Probes) or rhodamine Red-X-conjugated donkey anti-goat IgG (1 : 400; Jackson ImmunoResearch, West Grove, PA, USA). Sections were spread flat on slides, air dried and mounted with anti-fading medium Fluoromount-G (Southern Biotech, Birmingham, AL, USA) under coverslips. Images were collected using an Olympus FV300 confocal laser scanning microscope and processed with Adobe PHOTOSHOP 8.0 software.

For double staining using both antibodies derived from the same species (rabbit in this report), we followed the tyramide amplification method as described previously (Huang *et al.*, 2005). Briefly, on the first day, sections were incubated with PBST, followed by 3% hydrogen peroxide plus 10% methanol in PBST and then blocking solution as described above. The first primary antibody was applied overnight at a lower concentration than normally used. On the second day, with intervening washes with PBS, the signal for the first primary antibody was amplified sequentially by the biotinylated donkey anti-rabbit IgG (1 : 1000; Jackson ImmunoResearch), avidin-biotin-horseradish peroxidase complex (1 : 200), biotinylated tyramide (1 : 1000) and rhodamine Red-X-conjugated streptavidin (1 : 200; Jackson ImmunoResearch). The second primary antibody was then applied overnight at a normal concentration. On the third day, Alexa Fluor 488-conjugated donkey anti-rabbit IgG (1 : 500) was applied to visualize the second primary antibody. For Kv4.3/Kv4.2 or Kv4.3/Kv1.6 double labeling, sections were first processed for anti-Kv4.3 (1 : 800) and then anti-Kv4.2 (1 : 150) or anti-Kv1.6 (1 : 50).

Quantitative measurements

To measure the diameters of fluorescence-labeled Kv4.3(+) IG interneuron cell bodies, 30-μm transverse sections of spinal cords isolated from three P8 rats were used. The largest dimension of a fluorescence-labeled cell body could be visualized by changing the Z-axis of the confocal microscope. The average diameter was shown as the mean ± SEM (n = the number of experiments, the total number of cells measured).

To quantify the immunoreactivity (IR) of Kv4.2, Kv4.3 and Kv1.6 in the core region of IG, IR on a slide obtained from single antigen immunohistochemistry was transformed into an image with a Nikon DMX1200 digital camera connected to a Nikon Eclipse E800 light microscope and processed with Adobe PHOTOSHOP 8.0 software (for images from three rats at each developmental stage, see Supplementary material Figs S1–S3). Measurement of IR was then carried out by SCION IMAGE BETA 4.02 software (Scion, Frederick, MD, USA). The core region of IG (lamina VII) was circled and the IR within the circled area was measured as the sample value. A square area in the dorsal funiculus of the same section without obvious IR was chosen and measured as the background value. The ratio value was then obtained by dividing the sample value by the background value. After three images at a given developmental stage were measured, the average ratio value (mean ± SEM) was obtained (see Supplementary material, Tables S1–S3). The average ratio values at all developmental stages are plotted in Fig. 5. Each developmental stage was compared with the adult stage by Student's t-test to check whether there was a significant difference.

Results

Transient expression of Kv4.2 in somatic motoneurons

To check whether Kv4.2 is expressed in ventral horn neurons during E14–P8, we performed immunohistochemistry in rat spinal cord, from E12.5 through various developmental stages to adulthood. Kv4.2 IR first appeared in a cell cluster in the ventral part of ventral horn at E13.5 (Fig. 1A). Islet1/2 antibody recognizes both Islet1 and Islet2, which are two markers for immature postmitotic motoneurons. To verify whether Kv4.2(+) cells are motoneurons, Islet1/2 antibody was applied simultaneously for double immunofluorescent staining. Complete co-localization with Islet1/2 indicates that Kv4.2(+) cells are motoneurons (Fig. 4A). At the subcellular level, Kv4.2 IR appeared on the somatic surfaces of motoneurons only at E13.5 and on their processes at E14.5. Co-localization with MAP2 (a dendritic marker) indicates that Kv4.2(+) processes are dendrites (Fig. 4B). Based on the co-expression with Islet1/2 at E13.5 and the dendritic staining in the ventral horn during E14.5–17.5 (Fig. 1B), we reason that these Kv4.2(+) motoneurons are somatic motoneurons.

Peak expression of Kv4.2 in the somatic motoneurons was detected around E17.5 (Fig. 1B). Kv4.2 IR appeared in the dendritic field of all somatic motoneurons (Fig. 1B). However, Kv4.2 IR started to diminish from the lateral part of ventral horn after E17.5 and could be detected only from the ventral part at E19.5. Starting from E19.5, Kv4.2 IR also appeared in the dendrites of IG interneurons, which intermingled with Kv4.2 IR in the dendrites of somatic motoneurons. Nevertheless, because the diameter of motoneuron dendrites is larger than that of IG interneurons (Fig. 1C–H), we were still able to distinguish the dendritic staining in these two types of neurons. After birth, Kv4.2 IR in the motoneuron dendrites continued to decline (Fig. 1D and E) and became undetectable at P14 and in adulthood (Fig. 1G and H). Spinal motoneurons are generated during E11–14, with a peak at E12 in the cervical cord and at E13 in the lumbosacral cord. There is a rostro-to-caudal gradient in the development of somatic motoneurons. Besides the temporal order, we did not observe any rostro-caudal difference in Kv4.2 expression level or pattern at any developmental stage. In summary, Kv4.2 is transiently expressed in the somatodendritic domain of somatic motoneurons during E13.5–P8, with a peak around E17.5.

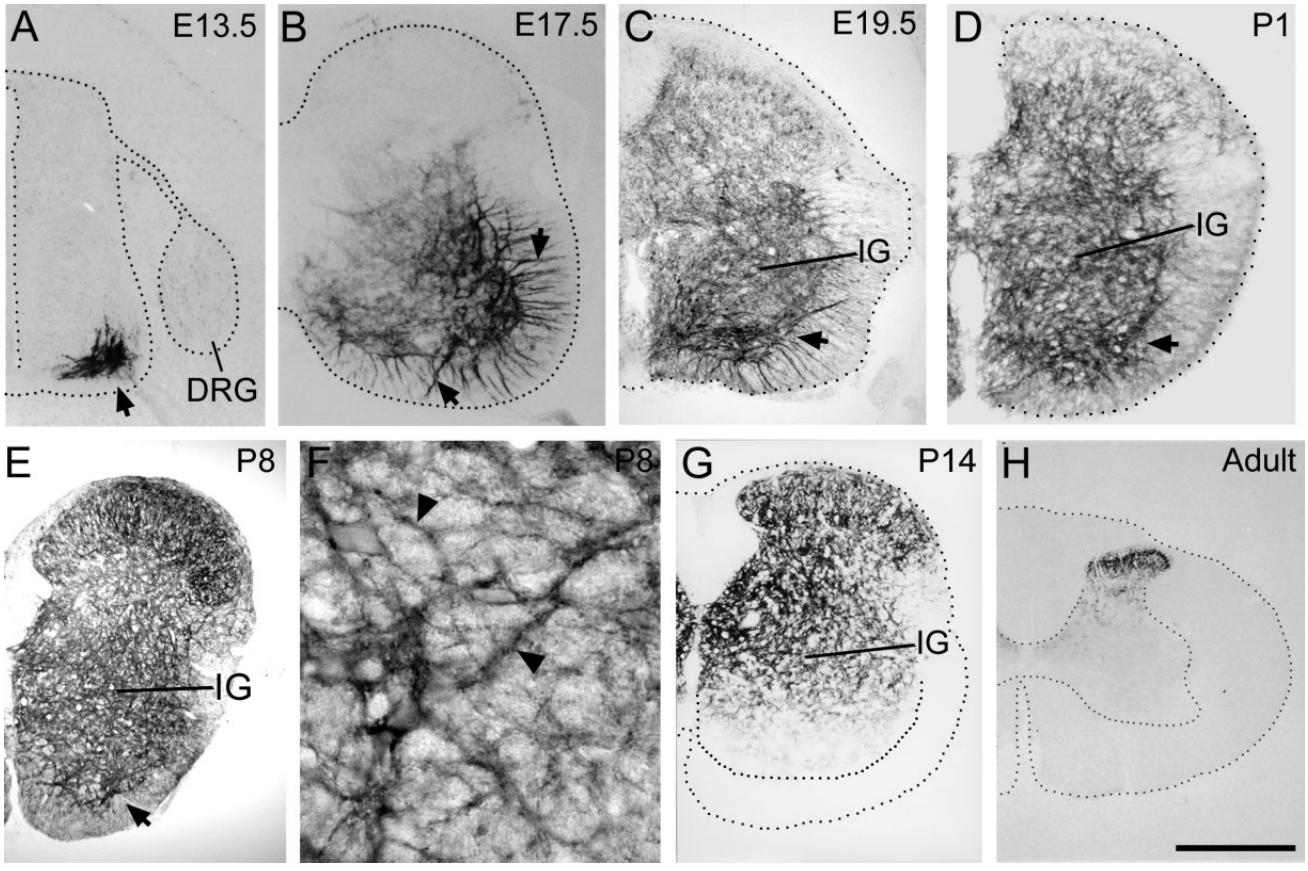

FIG. 1. Expression of Kv4.2 in rat spinal cord during development. Transverse sections at the cervical (except thoracic in A, D and E, and lumbar in G) level of spinal cord at various developmental stages as indicated were immunostained with Kv4.2 antibody. (A) At embryonic day (E) 13.5, Kv4.2 immunoreactivity (IR) is observed in the somatic motoneurons (arrow). (B) At E17.5, Kv4.2 IR has shifted from the cell bodies of somatic motoneurons to their dendrites (arrows), which sprout extensively in the ventral horn. (C) At E19.5, Kv4.2 IR in the somatic motoneurons has decreased and can be detected only in the ventral part of ventral horn (arrow). Kv4.2 IR first appears in the dendrites of intermediate gray (IG) interneurons. Although the dendritic staining of somatic motoneurons and IG interneurons intermingles within the ventral horn, the diameter of dendrites in the former is larger than in the latter. (D and E) At postnatal day (P) 1 and 8, Kv4.2 IR further decreases in the somatic motoneurons (arrows) but increases in the IG interneurons. (F) Higher magnification of Kv4.2 IR in the IG shown in E. Kv4.2 IR appears mainly in the dendrites of IG interneurons (arrowheads) instead of their somata. (G) At P14, Kv4.2 IR is barely detectable from the region occupied by somatic motoneurons. Its intensity in the IG is decreasing. (H) In adulthood, Kv4.2 IR has disappeared completely from the IG. Note that a transient expression of Kv4.2 in the somatic motoneurons during E13.5–P8 and in the IG interneurons during E19.5–P14. Scale bars, 210 μm (A and B); 250 μm (C); 150 μm (D); 375 μm (E); 58 μm (F); 390 μm (G); 750 μm (H). DRG, dorsal root ganglion.

Persistent expression of Kv4.3 in visceral motoneurons

To check whether Kv4.3 is expressed in the ventral horn neurons during E14–P8, we performed similar experiments as described for Kv4.2. Kv4.3 IR first appeared in the lateral and ventral parts of ventral horn at E13.5 (Fig. 2A). Similar patterns were observed from all spinal levels except the cervical cord. Co-expression with Islet1/2

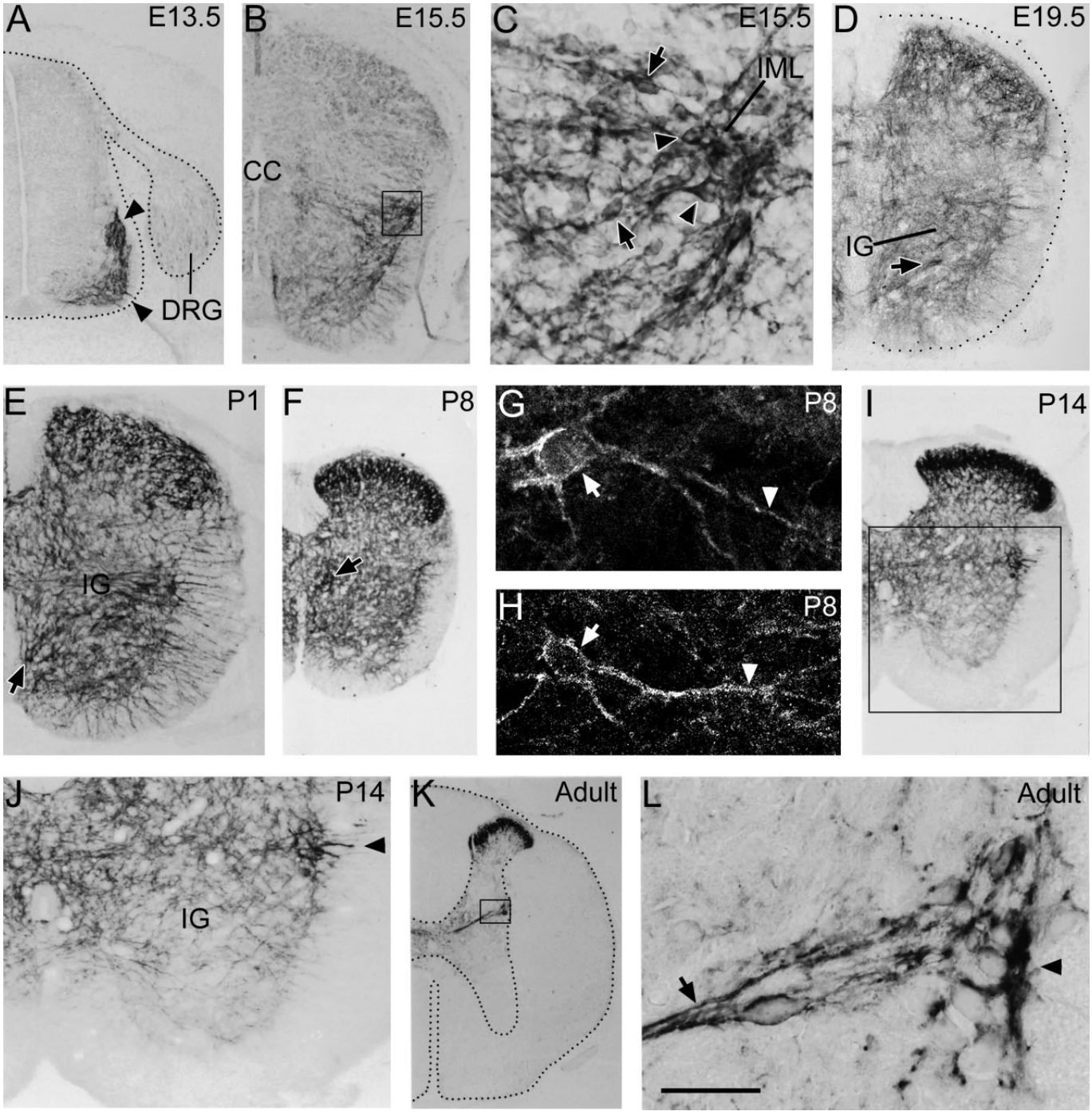

FIG. 2. Expression of Kv4.3 in rat spinal cord during development. Transverse sections at the thoracic level at various developmental stages as indicated were immunostained with Kv4.3 antibody. (A) At embryonic day (E) 13.5, Kv4.3 immunoreactivity (IR) first appears in the visceral motoneuron (arrowheads), which are migrating from the ventral horn toward the lateral horn. (B) At E15.5. (C) Higher magnification of the box in B. After Kv4.3(+) visceral motoneurons (arrowheads) have settled in the intermediolateral nucleus (IML) located in the lateral horn, some of them (arrows) further migrate medially toward the central canal (CC). (D) At E19.5, Kv4.3 IR first appears in a few intermediate gray (IG) interneurons (arrow). (E and F) At postnatal day (P) 1 and 8, many Kv4.3(+) IG interneurons (arrows) can be detected. (G and H) Confocal microscopic images of Kv4.3(+) IG interneurons at P8. Kv4.3 IR is obvious on their somatic surfaces (arrows) and dendrites (arrowheads). (I) At P14. (J) Higher magnification of the box in I, showing a reduction of Kv4.3 IR in the IG. Arrowhead indicates the Kv4.3(+) visceral motoneurons. (K) In adulthood, Kv4.3 IR remains apparent in the visceral motoneurons (box) but not in the IG. (L) Higher magnification of the box in K, showing Kv4.3 IR in the visceral motoneurons (arrowhead) and their dendrites extending horizontally (arrow). Note that Kv4.3 is expressed persistently in the visceral motoneurons during E13.5 to adulthood but transiently in the IG interneurons during E19.5–P14. Scale bars, 210 μm (A); 270 μm (B); 32 μm (C); 220 μm (D); 210 μm (E); 310 μm (F); 31 μm (G); 50 μm (H); 375 μm (I); 210 μm (J); 530 μm (K); 38 μm (L). DRG, dorsal root ganglion.

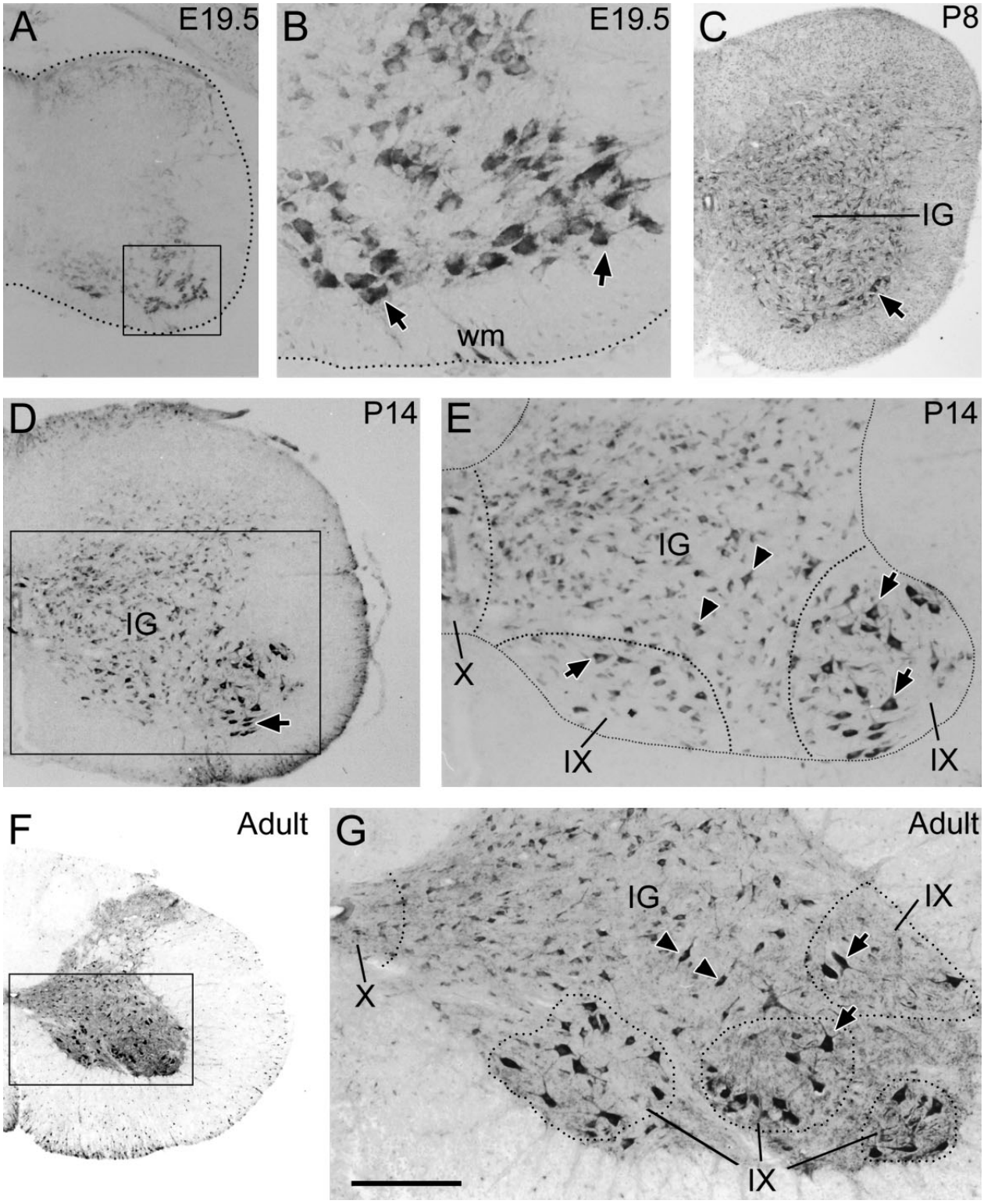

FIG. 3. Expression of Kv1.6 in rat spinal cord during development. Transverse sections at the cervical level at various developmental stages as indicated were immunostained with Kv1.6 antibody. (A) At embryonic day (E) 19.5, Kv1.6 immunoreactivity (IR) is obvious in the somatic motoneurons (box). (B) Higher magnification of the box in A, showing Kv1.6 IR in the cell bodies of somatic motoneurons (arrows). (C and D) At postnatal day (P) 8 and 14, in addition to somatic motoneurons (arrows), Kv1.6 IR also appears in a large number of interneurons scattered in the intermediate gray (IG). The intensity of Kv1.6 IR is stronger in the somatic motoneurons than IG interneurons. (E) Higher magnification of the box in D, showing Kv1.6(+) somatic motoneurons (arrows) in lamina IX (circled by dotted lines) and Kv1.6(+) IG interneurons (arrowheads). (F) In adulthood. (G) Higher magnification of the box in F, showing that Kv1.6 IR remains apparent in the somatic motoneurons (arrows) and IG interneurons (arrowheads). Note that Kv1.6 is persistently expressed in the somatic motoneurons and IG interneurons. Scale bars, 310 μm (A); 75 μm (B); 375 μm (C and D); 210 μm (E); 750 μm (F); 210 μm (G). wm, white matter.

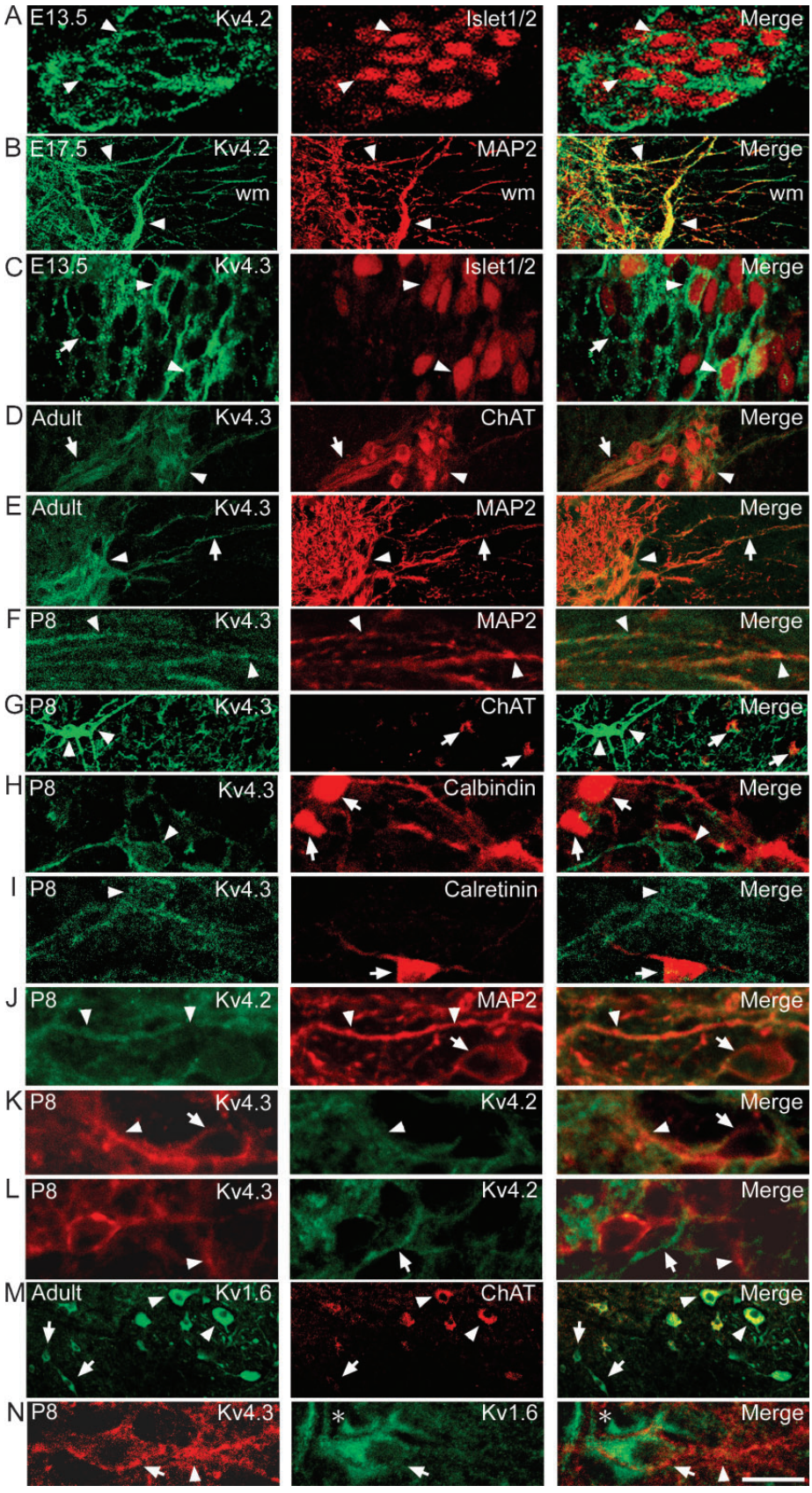

FIG. 4. Expression of Kv4.2, Kv4.3 and Kv1.6 in spinal motoneurons and intermediate gray (IG) interneurons during development. Transverse sections of rat spinal cord at various developmental stages as indicated were used for double immunofluorescent staining. (A) At embryonic day (E) 13.5, co-expression of Kv4.2 (green) and Islet1/2 (red) in the somatic motoneurons (arrowheads). Kv4.2 immunoreactivity (IR) is present on somatic surfaces, whereas Islet1/2 is in the cytoplasm. (B) At E17.5, co-existence of Kv4.2 (green) and microtubule-associated protein-2 (MAP2) (red) in the dendrites (arrowheads) of somatic motoneurons. (C) In E13.5 thoracic cord, some Kv4.3(+) visceral motoneurons (green) express Islet1/2 (red) (arrowheads) but some do not (arrow). (D) In adult thoracic cord, co-existence of Kv4.3 (green) and choline acetyltransferase (ChAT) (red) in the visceral motoneurons located in the intermediolateral nucleus (arrowhead) and intercalated region (arrow). (E) In adult thoracic cord, co-expression of Kv4.3 (green) and MAP2 (red) in the dendrites (arrow) of visceral motoneurons located in the intermediolateral nucleus (arrowhead). (F) At postnatal day (P) 8, co-localization of Kv4.3 (green) and MAP2 (red) in the dendrites (arrowheads) of some IG interneurons. (G) At P8, non-overlap between Kv4.3(+) (green, arrowheads) and ChAT(+) (red, arrows) IG interneurons. (H) At P8, non-overlap between Kv4.3(+) (green, arrowhead) and calbindin(+) (red, arrows) IG interneurons. (I) At P8, non-overlap between Kv4.3(+) (green, arrowhead) and calretinin(+) (red, arrows) IG interneurons. (J) At P8, co-localization of Kv4.2 (green) and MAP2 (red) in the dendrites (arrowheads) of many IG interneurons. MAP2 IR in the somata (arrow) is more obvious than Kv4.2 IR. (K) At P8, co-expression of Kv4.2 (green) and Kv4.3 (red) on the dendrites (arrowhead) of a small population of IG interneurons. Kv4.3 IR on the somatic surface (arrow) is more obvious than Kv4.2 IR. (L) In P8 lamina VII, both Kv4.2(+)/Kv4.3(–) (arrow) and Kv4.2(–)/Kv4.3(+) (arrowhead) dendrites can be seen. (M) In adult ventral horn, co-existence of Kv1.6 (green) and ChAT (red) in the somatic motoneurons (arrowheads). Arrows indicate Kv1.6(+)/ChAT(–) IG interneurons. (N) In P8 lamina VII, some Kv1.6(+) somata (green, arrow) show Kv4.3 IR (red) but most do not (star). Arrowhead indicates Kv4.3(+) dendrites. Scale bars, 15 μm (A); 63 μm (B); 17 μm (C); 58 μm (D); 74 μm (E); 33 μm (F); 83 μm (G); 38 μm (H); 24 μm (I); 11 μm (J); 20 μm (K); 18 μm (L); 100 μm (M); 21 μm (N). wm, white matter.

indicates that these Kv4.3(+) cells are motoneurons (Fig. 4C). Almost all Islet1/2(+) cells were Kv4.3(+) but only ~70% of Kv4.3(+) cells were Islet1/2(+). This is probably due to a significant down-regulation of Islet1 and Islet2 at this developmental stage (Tsuchida *et al.*, 1994; Thaler *et al.*, 2004). Kv4.3(+) motoneurons relocated to the lateral horn around E15.5 and clustered in the intermediolateral nucleus (IML) and the intercalated region (Fig. 2B and C). During development, in the thoracic, lumbar and sacral cords, visceral (or preganglionic) motoneurons first segregate in the ventral horn similar to somatic motoneurons and then migrate dorsally to the lateral horn to form the IML. Some of the visceral motoneurons further migrate along a horizontal route to the intercalated region (Phelps *et al.*, 1990; Altman & Bayer, 2001). Based on these data, we reason that Kv4.3(+) motoneurons are visceral motoneurons.

Kv4.3 IR in the visceral motoneurons remained detectable throughout development (Fig. 2E, I and J). In adulthood, Kv4.3 IR was obvious in a cluster of cells located in the IML and the horizontally oriented processes extending toward the central canal (Fig. 2K and L). ChAT has been used as another marker for motoneurons in the mature stage and the immature stage later than Islet1/2 (Barber *et al.*, 1984). Co-localization of Kv4.3 and ChAT in the IML and the intercalated region confirms that Kv4.3 is still expressed in the visceral motoneurons in adulthood (Fig. 4D). Co-localization with MAP2 in the processes extending out from the IML indicates that Kv4.3 is present on the dendrites of visceral motoneurons (Fig. 4E). At the subcellular level, Kv4.3 is present in the somatic surfaces of visceral motoneurons during E13.5–15.5 and appears in both the somata and dendrites after E15.5 and throughout adulthood. In summary, Kv4.3 is persistently expressed in the somatodendritic domain of visceral motoneurons, after E13.5 and throughout adulthood.

Transient expression of Kv4.3 in a subset of intermediate gray interneurons

The field of IG extends to the base of dorsal horn and penetrates the interstices of ventral horn unoccupied by somatic motoneurons (lamina IX), i.e. including laminae IV–VIII (Parent, 1996; Altman & Bayer, 2001). Most of the IG, except for the discrete cells grouping as Clarke's column near the central canal, the intercalated region and the IML of the lateral horn, is composed of many small- and mid-sized interneurons. In the IG, Kv4.3 IR first appeared at E19.5 (Fig. 2D), reached a peak around P1 (Fig. 2E), remained at high level at P8 (Fig. 2F), followed by a decline at P14 (Fig. 2I and J) and became undetectable in adulthood (Fig. 2K). Kv4.3 IR could be detected from the IG at all spinal levels during E19.5–P14 (Fig. 2).

Kv4.3 IR on the somatic surfaces and processes of certain IG interneurons could be most clearly seen at P8 (Fig. 2G and H). Co-localization with MAP2 indicates that the processes are dendrites (Fig. 4F). The majority of Kv4.3(+) IG interneurons have multipolar cell bodies, with three to four dendritic trunks, which give rise to only a few side branches but cover a wide area of the spinal gray matter. The average diameter of Kv4.3(+) interneuron cell bodies was 24.4 ± 4.0 μm ($n = 7$; 21 cells) at P8. To further characterize the Kv4.3(+) IG interneurons, double staining was performed with ChAT (a marker for cholinergic interneurons; Barber *et al.*, 1984), calbindin (a marker for Renshaw cells) or calretinin (Zhang *et al.*, 1990; Ren &

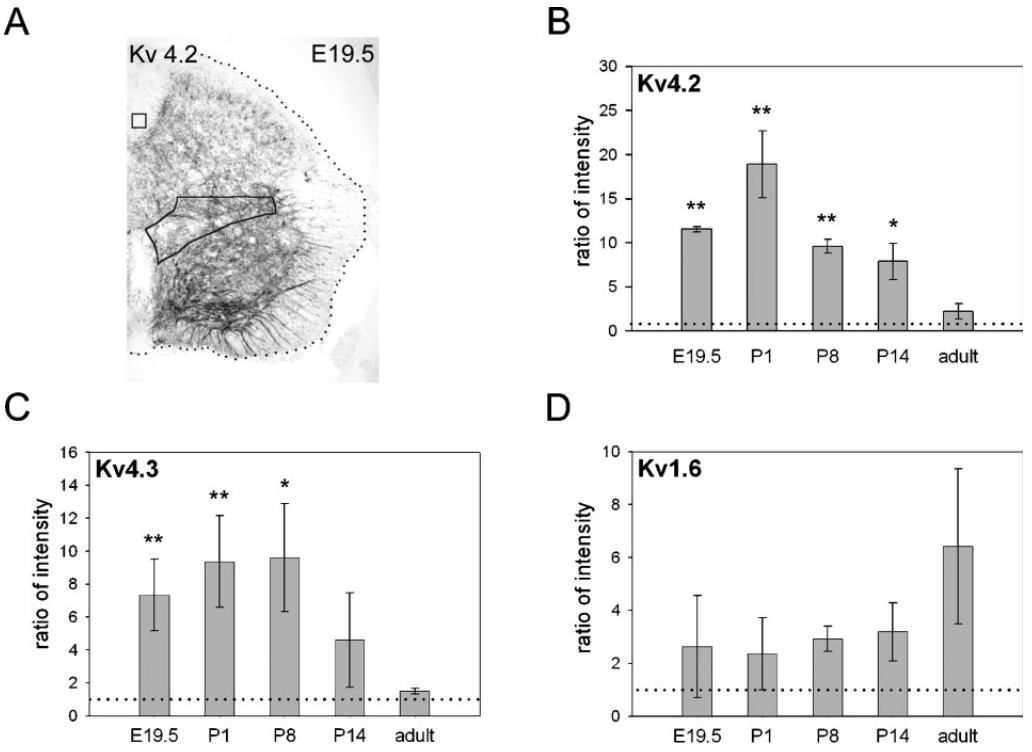

FIG. 5. Quantitative analysis of Kv4.2, Kv4.3 and Kv1.6 expression in spinal cord lamina VII during development. (A) A representative image [Kv4.2 in the cervical cord at embryonic day (E) 19.5] is shown for quantification. The immunoreactivity (IR) in the core region of intermediate gray (lamina VII) was circled and measured as the sample value and the IR within a square in the dorsal funiculus was measured as the background value. The ratio of intensity was obtained by dividing the sample value by the background value and a ratio value of 1 (horizontal dotted lines) indicates that the IR in lamina VII is the same as the background. After three images at a given stage were measured, the average ratio (mean ± SEM) was obtained and plotted in B for Kv4.2, C for Kv4.3 and D for Kv1.6. Comparing with adulthood, a significant increase of Kv4.2 IR and Kv4.3 IR was detected during E19.5 to postnatal day (P) 14, with a peak at approximately P1. In contrast, moderate to low levels of Kv1.6 IR appeared at all stages without obvious change. *$P < 0.05$, **$P < 0.01$, comparing each developmental group with adult group by Student's *t*-test.

Ruda, 1994). Our results indicate that Kv4.3(+) IG interneurons are ChAT(–)/calbindin(–)/calretinin(–) (Fig. 4G–I). In summary, during E19.5–P14, Kv4.3 is transiently expressed in the somatodendritic domain of a subset of IG interneurons.

Transient expression of Kv4.2 in another subset of intermediate gray interneurons

Kv4.2 IR could also be detected from the IG at all spinal levels during E19.5–P14 (Fig. 1), similar to Kv4.3. Kv4.2 IR in the IG first appeared at E19.5 (Fig. 1C), reached a peak around P1 (Fig. 1D), remained at high level at P8 (Fig. 1E), followed by a decline at P14 (Fig. 1G) and became undetectable in adulthood (Fig. 1H). During E19.5–P14, Kv4.2 IR was apparent only in the processes (Fig. 1F) and co-localization with MAP2 indicates that the processes are dendrites (Fig. 4J).

To check whether Kv4.2 is expressed in the dendrites of Kv4.3(+) IG interneurons, double immunostaining with tyramide amplification was performed. Based on the overlap of dendritic staining, we found that there was a subset of Kv4.2(+) IG interneurons, a subset of Kv4.3(+) IG interneurons and a smaller subset of Kv4.2(+)/Kv4.3(+) IG interneurons (Fig. 4K and L). As Kv4.2 IR appeared only in the dendrites, we were unable to characterize the subset of Kv4.2(+) IG interneurons using markers labeling mainly on the somata. In summary, during E19.5–P14, Kv4.2 is transiently expressed in the dendrites of a subset of IG interneurons, among which a smaller subset also express Kv4.3 in their dendrites and somata.

Persistent expression of Kv1.6 in somatic motoneurons and intermediate gray interneurons

We also examined the expression of Kv1.6 in the ventral horn during development for comparison. Kv1.6 IR became obvious in the somatic motoneurons at E19.5 (Fig. 3A and B). At P8, Kv1.6 IR also appeared in the IG interneurons (Fig. 3C). At P14 and in adulthood, Kv1.6(+) somatic motoneurons became much larger and stronger in intensity than Kv1.6(+) IG interneurons (Fig. 3D–G). Kv1.6 was localized mainly in the cytoplasm in both types of neurons. Co-localization with ChAT confirms that Kv1.6 is present in somatic motoneurons (Fig. 4M). In addition, a small subset of Kv1.6(+) IG interneurons co-expressed Kv4.3 (Fig. 4N). In summary, during development and throughout adulthood, Kv1.6 is persistently expressed in the cytoplasm of somatic motoneurons and IG interneurons.

Quantitative analysis in intermediate gray interneurons

To quantify the changes in Kv4.2, Kv4.3 and Kv1.6 expression in the IG interneurons during development, we applied an image analysis. To avoid overlapping with the dendritic staining of somatic motoneurons, only the area corresponding to the core of IG (lamina VII) was measured (Fig. 5A). The statistical data are shown in Fig. 5B–D (also see Supplementary material, Tables S1–S3). In the core region of IG, Kv4.2 IR became obvious at E19.5, increased greatly at P1, slowly declined at P8 and 14 and returned to a background level in adulthood (Fig. 5B). Kv4.3 IR shows a similar pattern as Kv4.2 IR (Fig. 5C). At the peak expression stage (P1), the intensity of Kv4.2 IR was approximately two-fold that of Kv4.3 IR (Fig. 5B and C). In contrast, moderate to low levels of Kv1.6 IR could be detected persistently from lamina VII and there was no significant difference between adult and individual developmental stages (Fig. 5D).

Discussion

Three main findings arise from this study. Firstly, Kv4.2 is transiently expressed in the somatic motoneurons during E13.5–P8, with a peak around E17.5. Secondly, Kv4.2 and Kv4.3 are transiently expressed in different subsets of IG interneurons during E19.5–P14, with a peak around P1. In contrast, the delayed rectifier K^+ current-expressing subunit Kv1.6 is persistently expressed in the somatic motoneurons and IG interneurons. Thirdly, Kv4.3 is persistently expressed in the visceral motoneurons after E13.5 and throughout adulthood.

Correlations between A-type K^+ currents and immunostaining data

Using whole cell patch-clamp recording in rat spinal cord slices, I_As have been detected from the somatic motoneurons in E15–16, P1–3 (Safronov & Vogel, 1995), P2–8 (Gao & Ziskind-Conhaim, 1998) and E14 rat motoneuron cultures (Alessandri-Haber *et al.*, 1999). In this study, we have observed, by immunohistochemistry, Kv4.2 in the somatic motoneurons during E13.5–P8, consistent with previous electrophysiological data *in vivo* and *in vitro*. I_As have also been recorded from visceral motoneurons in a neonatal period (P7–13; Miyazaki *et al.*, 1996) and in young adulthood (P21–28; Sah & McLachlan, 1995). We have consistently found a persistent expression of Kv4.3, which starts from E13.5 and continues throughout adulthood. In addition, Kv4.2 and Kv4.3 were detected from their somatodendritic domain, which is consistent with the electrophysiological data reported. Thus, it is likely that Kv4.2 and Kv4.3 are the main I_A contributors in the somatodendritic domain of these motoneurons. Nevertheless, the possibility that the other I_A-expressing subunits (Kv1.4, Kv3.4 and Kv4.1) are also involved has not been excluded.

Our immunostaining data indicate that Kv4.2 and Kv4.3 are transiently expressed in the IG interneurons during E19.5–P14. Kv4.3 is expressed in the somata and dendrites of a subset of IG interneurons, which are Kv1.6(+)/ChAT(–)/calbindin(–)/calretinin(–). Kv4.2 is expressed mainly in the dendrites of another subset of IG interneurons. Co-localization of Kv4.2 and Kv4.3 could be detected from the dendrites of a smaller subset of IG interneurons. Whether the other I_A-expressing subunits (Kv1.4, Kv3.4 and Kv4.1) are also expressed in the IG interneurons during development remains to be examined. However, so far no I_A has been reported from the IG interneurons during development. This might be due to the short time window (E19.5–P14) and the diversity of IG interneurons. Nevertheless, our finding provides an initial step toward understanding the transient I_A-expressing IG interneurons.

Possible function for transient expression of Kv4.2 in somatic motoneurons

In the rat, motoneurons are generated during E11–14 (Altman & Bayer, 2001). However, the number of somatic motoneurons is reduced by a process of naturally occurring apoptosis and ~50% of motoneurons undergo cell death during E15–17 (Harris & McCaig, 1984). It has been found that cell death increases with motoneuron excitability. In other words, blocking neuronal activity increases survival, whereas increasing neuronal activity decreases survival. As I_A can counterbalance the increasing excitability developed during the period of developmental selection, it has been hypothesized that individual motoneurons could be spared from apoptosis by the expression of I_A (McCobb *et al.*, 1990). Coincident with the period of developmental selection, we observed a peak expression of Kv4.2 in

the somatic motoneurons around E17.5. Our data support the hypothesis that increase of I_A may protect I_A-expressing motoneurons from apoptosis.

Possible function for transient expression of Kv4.2 and Kv4.3 in intermediate gray interneurons

Intermediate gray interneurons, which are targets of proprioceptive and exteroceptive fibers, directly (monosynaptically) or indirectly (polysynaptically) regulate the excitability of somatic motoneurons (Altman & Bayer, 2001). In the rat, IG interneurons are generated 1–2 days later than motoneurons. Similar to motoneurons, IG interneurons also undergo apoptosis, which occurs around birth. Nevertheless, the proportion of IG interneurons undergoing apoptosis is smaller compared with that of somatic motoneurons (reviewed in Lowrie & Lawson, 2000). We have shown a significant increase of Kv4.2 and Kv4.3 expression in the IG interneurons around birth, which coincides with the time of IG interneuron apoptosis. Based on the close relationship between somatic motoneurons and IG interneurons, it is possible that the increase of I_As by Kv4.2 and Kv4.3 expression may protect I_A-expressing IG interneurons from apoptosis, a mechanism similar to that proposed for the somatic motoneurons.

Supplementary material

The following supplementary material may be found on http://www.blackwell-synergy.com

Fig. S1. Kv4.2 expression at five developmental stages.

Fig. S2. Kv4.3 expression at five developmental stages.

Fig. S3. Kv1.6 expression at five developmental stages.

Table S1. Quantitative analysis of Kv4.2 expression in lamina VII during development.

Table S2. Quantitative analysis of Kv4.3 expression in lamina VII during development.

Table S3. Quantitative analysis of Kv1.6 expression in lamina VII during development.

Acknowledgements

We are grateful to Hirou Kaneshige, Dr Fu-Chin Liu and Dr Wen-Lin Liao for their technical support. This work was supported by a grant (NSC 93-2320-B-010-045) from the National Scientific Council (Taiwan, ROC) and a grant (MMHYM 94-011) from the Joint Research Program of Mackay Memorial Hospital and National Yang-Ming University.

Abbreviations

ChAT, choline acetyltransferase; E, embryonic day; I_A, A-type K^+ current; IG, intermediate gray; IML, intermediolateral nucleus; IR, immunoreactivity; MAP2, microtubule-associated protein-2; P, postnatal day; PBS, phosphate-buffered saline; PBST, phosphate-buffered saline containing 0.3% Triton X-100.

References

Alessandri-Haber, N., Paillart, C., Arsac, C., Gola, M., Couraud, F. & Crest, M. (1999) Specific distribution of sodium channels in axons of rat embryo spinal motoneurons. *J. Physiol.*, **518**, 203–214.

Alessandri-Haber, N., Alcaraz, G., Deleuze, C., Jullien, F., Manrique, C., Couraud, F., Crest, M. & Giraud, P. (2002) Molecular determinants of emerging excitability in rat embryonic motoneurons. *J. Physiol.*, **541**, 25–39.

Altman, J. & Bayer, S.A. (2001) *Development of the Human Spinal Cord*. Oxford University Press, New York, N.Y.

Barber, R.P., Phelps, P.E., Houser, C.R., Crawford, G.D., Salvaterra, P.M. & Vaughn, J.E. (1984) The morphology and distribution of neurons containing choline acetyltransferase in the adult rat spinal cord: an immunocytochemical study. *J. Comp. Neurol.*, **229**, 329–346.

Birnbaum, S.G., Varga, A.W., Yuan, L.L., Anderson, A.E., Sweatt, J.D. & Schrader, L.A. (2004) Structure and function of Kv4-family transient potassium channels. *Physiol. Rev.*, **84**, 803–833.

Coetzee, W.A., Amarillo, Y., Chiu, J., Chow, A., Lau, D., McCormack, T., Moreno, H., Nadal, M.S., Ozaita, A., Pountney, D., Saganich, M., Vega-Saenz De Miera, E. & Rudy, B. (1999) Molecular diversity of K^+ channels. *Ann. N.Y. Acad. Sci.*, **868**, 233–285.

Gao, B.X. & Ziskind-Conhaim, L. (1998) Development of ionic currents underlying changes in action potential waveforms in rat spinal motoneurons. *J. Neurophysiol.*, **80**, 3047–3061.

Harris, A.J. & McCaig, C.D. (1984) Motoneurons death and motor unit size during embryonic development of the rat. *J. Neurosci.*, **4**, 13–24.

Hille, B. (2001) *Ion Channels of Excitable Membranes*, 3rd Edn. Sinauer Associates, Sunderland, MA.

Hsu, Y.H., Huang, H.Y. & Tsaur, M.L. (2003) Contrasting expression of Kv4.3, an A-type K^+ channel, in migrating Purkinje cells and other post-migratory cerebellar neurons. *Eur. J. Neurosci.*, **18**, 601–612.

Huang, H.Y., Cheng, J.K., Shih, Y.H., Chen, P.S., Wang, C.L. & Tsaur, M.L. (2005) Expression of A-type K^+ channel α subunits Kv4.2 and Kv4.3 in rat spinal lamina II excitatory interneurons and co-localization with pain-modulating molecules. *Eur. J. Neurosci.*, **22**, 1149–1157.

Lowrie, M.B. & Lawson, S.J. (2000) Cell death of spinal interneurons. *Prog. Neurobiol.*, **61**, 543–555.

McCobb, D.P., Best, P.M. & Beam, K.G. (1990) The differentiation of excitability in embryonic chick limb motoneurons. *J. Neurosci.*, **10**, 2974–2984.

Miyazaki, T., Dun, N.J., Kobayashi, H. & Tosaka, T. (1996) Voltage-dependent potassium currents of sympathetic preganglionic neurons in neonatal rat spinal cord thin slices. *Brain Res.*, **743**, 1–10.

Parent, A. (1996) *Carpenter's Human Neuroanatomy.* William and Wilkins, Baltimore, PA.

Perrier, J.F. & Hounsgaard, J. (2000) Development and regulation of response properties in spinal cord motoneurons. *Brain Res. Bull.*, **53**, 529–535.

Phelps, P.E., Barber, R.P., Brennan, L.A., Maines, V.M., Salvaterra, P.M. & Vaughn, J.E. (1990) Embryonic development of four different subsets of cholinergic neurons in rat cervical spinal cord. *J. Comp. Neurol.*, **291**, 9–26.

Pongs, O. (1999) Voltage-gated potassium channels: from hyperexcitability to excitement. *FEBS Lett.*, **452**, 31–35.

Ren, K. & Ruda, M.A. (1994) A comparative study of the calcium-binding proteins calbindin-D28K, calretinin, calmodulin and parvalbumin in the rat spinal cord. *Brain Res.*, **19**, 163–179.

Rhodes, K.J., Carroll, K.I., Sung, M.A., Doliveira, L.C., Monaghan, M.M., Burke, S.L., Strassle, B.W., Buchwalder, L., Menegola, M., Cao, J., An, W.F. & Trimmer, J.S. (2004) KChIPs and Kv4 α subunits as integral components of A-type potassium channels in mammalian brain. *J. Neurosci.*, **24**, 7903–7915.

Safronov, B.V. & Vogel, W. (1995) Single voltage-activated Na^+ and K^+ channels in the somata of rat motoneurones. *J. Physiol.*, **487**, 91–106.

Sah, P. & McLachlan, E.M. (1995) Membrane properties and synaptic potentials in rat sympathetic preganglionic neurons studied in horizontal spinal cord slices *in vitro*. *J. Auton. Nerv. Syst.*, **53**, 1–15.

Thaler, J.P., Koo, S.J., Kania, A., Lettieri, K., Andrews, S., Cox, C., Jessell, T.M. & Pfaff, S.L. (2004) A postmitotic role for Isl-class LIM homeodomain proteins in the assignment of visceral spinal motor neuron identity. *Neuron*, **41**, 337–350.

Toledo-Rodriguez, M., Manira, A.E., Wallen, P., Svirskis, G. & Hounsgaard, J. (2005) Cellular signalling properties in microcircuits. *Trends Neurosci.*, **28**, 534–540.

Tsuchida, T., Ensini, M., Morton, S.B., Baldassare, M., Edlund, T., Jessell, T.M. & Pfaff, S.L. (1994) Topographic organization of embryonic motor neurons defined by expression of LIM homeobox genes. *Cell*, **79**, 957–970.

Veh, R.W., Lichtinghagen, R., Sewing, S., Wunder, F., Grumbach, I.M. & Pongs, O. (1995) Immunohistochemical localization of five members of the Kv1 channel subunits: contrasting subcellular locations and neuron specific co-localizations in rat brain. *Eur. J. Neurosci.*, **7**, 2189–2205.

Zhang, J.H., Morita, Y., Hironaka, T., Emson, P.C. & Tohyama, M. (1990) Ontological study of calbindin-D_{28k}-like and parvalbumin-like immunoreactivities in rat spinal cord and dorsal root ganglia. *J. Comp. Neurol.*, **302**, 715–728.